Academic Journal of Emerging Technologies
ISSN Print: 3104-4417
ISSN Online: 3104-4425
CD ISSN: 3104-4433
https://doi.org/10.63313/AJET.9018

The Synergistic Effect of Waterjet Assistance and a Novel Line-Delay Strategy on Precision Laser Drilling of Inconel 718

Xuecheng Gao[1,2]. Shufeng Sun[1,2,*]. Jin Wang[1,2*]. Fengyun Zhang[1,2]. Yaofei Ma[1,2]. Tao Wei[1,2]. Junbao Li[1,2] and Pingping Wang[1,2]
[1]Discipline Innovation and Wisdom Introduction Base of High-end Laser Intelligent Manufacturing Technology and Equipment, school of Mechanical and Automotive Engineering, Qingdao University of Technology, Qingdao 266520, China
[2]Key Laboratory of High-end Laser Manufacturing Technology and Equipment of Shandong Province, school of Mechanical and Auto-motive Engineering, Qingdao University of Technology, Qingdao 266520, China
Email: sunshufeng@qut.edu.cn

How to cite this paper: Gao, X. C., Sun, S. F., Wang, J., Zhang, F. Y., Ma, Y. F., Wei, T., Li, J. B., & Wang, P. P. (2025). The Synergistic Effect of Waterjet Assistance and a Novel Line-Delay Strategy on Precision Laser Drilling of Inconel 718. *Academic Journal of Emerging Technologies*, 1(3), 18-27. ISSN Print: 3104-4417; ISSN Online: 3104-4425.
https://doi.org/10.63313/AJET.9018
Published: 2025-11-05

Abstract

This study investigates the optimization of process parameters for water-jet-assisted nanosecond laser drilling of Inconel 718, with a focus on improving microhole quality through pulse delay strategies and defocus control. Expe-ri-ments were conducted using concentric circular scanning under both under-wa-ter and in-air conditions, with emphasis on the effects of delay meth-ods—specifically face-delay and line-delay—on geometric accuracy and mor-phologi-cal integrity. Results indicate that the line-delay approach significantly reduces entrance diameter, taper, microcracks, and oxidation compared to non-delayed and face-delayed conditions. The ablation threshold increased from 12.58 J/cm^2 in air to 22.12 J/cm^2 underwater due to energy attenuation effects. Optimal machining quality was achieved with a defocus distance of −0.5 mm, cor-re-sponding to focal positioning near the workpiece center. The study de-mon-strates that waterjet-assisted laser drilling with adaptive pulse delay effec-tively enhances machining precision and surface quality, showing great potential for applications in high-temperature component manufacturing.

Keywords

Laser drilling; waterjet assistance; pulse delay; Inconel 718; process optimization; microhole quality

1. Introduction

Nickel-based superalloys are widely employed in high-temperature environments such as aero-engine turbine blades and hot-section components of gas turbines due to their excel-lent high-temperature strength, oxidation resistance, and corrosion resistance [1]. The machining quality of micro-hole structures (e.g., film cooling holes) in these components directly affects the heat dissipation efficiency and service life of the parts. However, these alloys are considered typical difficult-to-machine materials owing to their high hardness, high melting point, and low thermal conductivity [2]. Therefore, it is of great significance to develop high-quality and high-efficiency micro-hole machining processes.

Currently commonly used micro-hole machining techniques mainly include mechanical drilling [3], electrical discharge machining (EDM) [4], electrochemical machining (ECM) [5], and laser drilling [6]. Mechanical drilling is prone to drill breakage, making it difficult to achieve stable micro-hole processing [7]; EDM suffers from a large heat-affected zone, recast layer, and micro-cracks, and is limited to conductive materials [8]; ECM is free of thermal stress but affected by stray corrosion, making it unsuitable for micro-holes below 0.8 mm in diameter [9]. Traditional laser processing (especially in air), though featuring non-contact and high efficiency, still faces issues such as micro-cracks, slag adhesion, and heat-affected zones due to heat accumulation [10]. Ultra-short pulse lasers can significantly suppress thermal damage, achieving near-"cold processing", but their high equipment costs and low efficiency limit industrial applications.

To improve laser drilling quality, liquid-assisted laser processing techniques have emerged, among which water-assisted laser drilling is the most representative. This technique involves covering the workpiece surface with a water medium or forming a water jet to guide the laser. Utilizing the flushing action and cooling effect of water on molten material, it significantly reduces the recast layer, heat-affected zone, and micro-cracks, thereby improving hole wall quality and machining accuracy. Zhang et al. proposed a composite water-assisted method combining spray water film with backflow, which effectively carried away heat and slag during processing, significantly improving the exit morphology and roundness of holes in nickel-based alloys [11]. Additionally, the water layer can suppress plasma splashing, reduce hole burrs, and improve processing consistency.

Compared to other auxiliary processing methods (such as magnetic field [12], ultrasonic [13], and multi-energy field composite assistance [14]), water-assisted laser drilling offers advantages including simple setup, low cost, and strong applicability, making it easier to integrate into industrial-grade laser equipment and demonstrating good prospects for engineering application. Beyond process optimization, researchers have also been devoted to developing path planning and pulse control strategies (such as dual-pulse [15] and dual-path scanning [16]) in recent years, further enhancing the geometric accuracy and repeatability of water-assisted laser drilling.

This paper focuses on the application of water-assisted laser drilling technology in the micro-hole processing of nickel-based superalloys. It systematically investigates the effects of different water layer conditions, laser parameters, and scanning strategies on micro-hole formation quality, and explores the regulatory mechanism of water medium in the laser ablation process. The aim is to provide a process basis and theoretical support for achieving high-precision, low-damage, and high-efficiency micro-hole machining.

2. Experimental design

The experimental material used in this study was Inconel 718, with dimensions of 20 mm × 20 mm × 1 mm, a nickel-based superalloy commonly employed in aircraft engine turbine blades due to its superior mechanical properties at elevated temperatures. The principal constituent elements of this alloy include nickel (Ni), chromium (Cr), iron (Fe), and niobium (Nb).

A nanosecond pulsed laser processing system with a wavelength of 1064 nm was utilized, incorporating an IPG ytterbium-doped pulsed fiber laser source. Key laser parameters comprise a maximum average power of 200 W, a beam quality factor of $M^2 < 1.3$, a pulse duration of 100 ns, and a repetition rate adjustable from 20 kHz to 2000 kHz. This type of fiber laser is well-suited for processing various metals, polymers, and ceramics. A schematic of the nanosecond laser processing setup is illustrated in Fig. 1. The infrared laser beam first passes through a collimating lens to generate a collimated beam, which is then directed by a mirror-based beam delivery system to a galvanometer scanner. The scanner deflects the beam precisely according to the pre-programmed machining path, enabling the beam to be focused onto the workpiece surface through an F-theta lens. The resulting focused spot diameter on the workpiece is approximately 64 μm.

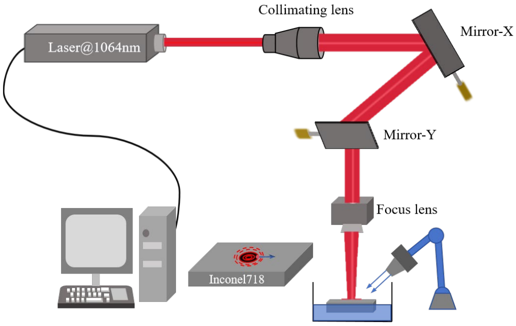

Figure 1. Schematic diagram of nanosecond laser processing.

3. Results and discussions

This study examined waterjet-assisted nanosecond laser drilling of Inconel 718, focusing on how pulse delay strategies improve microhole quality. During processing, a waterjet formed a thin film over the workpiece, enabling the laser to act through it while the flowing water efficiently cleared debris from the hole walls.

3.1. Optimization of Pulse-Delay Strategy

Based on two delayed scanning strategies, the experiment employed concentric circular scanning for micro-hole processing, as illustrated in Fig. 2(a). The laser follows an inward spiral trajectory with constant radial spacing. In the layer-by-layer approach (Fig. 2(b)), after completing each full layer of concentric circles, a fixed pulse-delay is inserted before starting the next layer. This method uses an equal-pulse-delay strategy and is referred to as face-delay.

An upgraded strategy, termed line-delay, addresses the limitations of face-delay. As concentric circles decrease in diameter, the processing time and required pulse count per ring vary. Applying a fixed pulse-delay may interrupt ring completion, leading to random crater formation and reduced roundness. Thus, an adaptive delay strategy is implemented based on the processing time of each individual ring rather than pulse count. As shown in Fig. 2(c), after finishing one full ring (e.g., time t1 for the outermost circle), a delay interval t is introduced before proceeding inward. This cycle repeats from the outermost ring until all specified scans are completed.

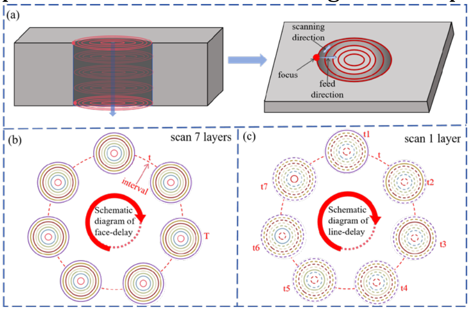

Figure 2. Schematic diagram of laser pulse-delay machining scanning principle: (a) Number of scanning n times, concentric ring scanning from outside to inside; (b) face-delay after completing each concentric ring; (c) Line-delay after completing each concentric ring.

The variation rule of the number of pulses with the processing time is shown in Fig. 3.(a). In the case of no-delay, the number of pulses increases linearly with the processing time due to the fixed repetition frequency. And after the use of pulse-delay, the addition of delay time interval will directly affect the total processing time, mainly dependent on the length and number of the delay intervals. The number of pulses output per unit time without delay is greater than that with face-delay, which in turn is greater than that with line-delay. Specifically, in the no-delay state, the pulse output is continuous and stable, and the number of pulses per unit time is the largest; with face-delay introduces a fixed delay time between each set of pulses, and although the pulse frequency remains unchanged, the intervals between the pulse outputs increase the total machining time, resulting in a slightly lower number of pulses per unit time than in the no-delay state, with the number of pulse intervals determined by the number of times of machining operations, and the length of the time interval can be autonomously set. With line-delay, the number of pulse intervals is further increased, resulting in the slowest increase in the number of pulses, and therefore the lowest number of pulses per unit time, and the number of pulse intervals is determined by the fill spacing and the number of scans together.

The variation rule of inlet diameter with the number of pulses is shown in Fig. 3.(b). The no-delay inlet diameter is the largest and increases gradually with the number of pulses. The face-delay introduces a pulse interval, and the inlet diameter is slightly smaller than that of the no-delay state, but the difference is not significant, which should be caused by the smaller time interval. In contrast, the entrance diameter of the line-delay is greatly reduced and stabilized at about 460 μm, which is greatly reduced compared with the other two methods. The line-delay plays an effective role in precisely regulating the time interval between each group of laser pulse trains, controlling the action time of the laser energy on the surface of the material, significantly reducing the heat accumulation, and preventing the material from over-melting and diffusing outward, thus optimizing the size of the micro-holes.The change rule of processing depth with the number of pulses is shown in Fig. 3. (c). In the line-delayed state, the laser processing depth is almost linear with the number of pulses until a through-hole is formed. With the increase in the number of pulses, the processing depth gradually increases, and the longitudinal removal is more obvious. The pulse output rate without delay is higher, requiring close to 8000 pulses for the material to achieve through-hole, and a high volume of molten material before the through-hole is formed, and the flow irregularities impede the formation of the through-hole. The variation rule of the cross-sectional area with the number of pulses is shown in Fig. 3. (d), where the cross-sectional area of both no-delay and face-delay is expanded to different degrees, eventually up to more than 500000 μm^2 , while the line-delay controls the overall energy, making the micro-hole area eventually float at 400000 μm^2 , which is the closest to the ideal state.

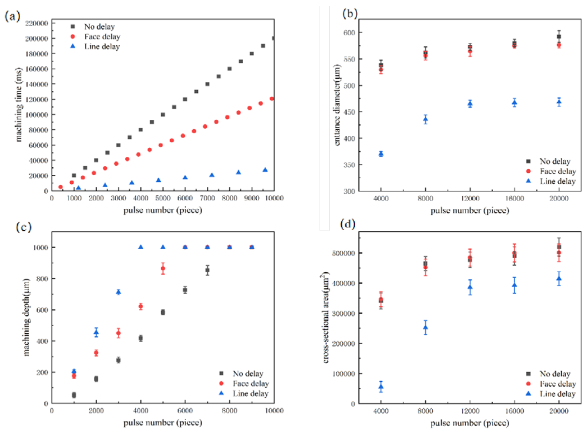

Figure 3. Comparison of three laser machining states (no-delay, face-delay, line-delay): (a) Change in pulse number with machining time; (b) Change in entrance diameter with pulse number; (c) Change in machining depth with pulse number; (d) Change in cross-sectional area with pulse number.

3.2. Optimization of water-assisted laser process parameters

The ablation threshold of IN718 alloy was investigated through single-pulse ablation experiments conducted in both underwater and in-air environments. The ablation threshold is defined as the minimum energy density required to initiate material damage and removal. Experiments were performed in single-pulse mode with a pulse duration of 100 μs, a repetition rate of 20 kHz, and a water layer thickness of 0.3 mm. The laser power was varied from 80 W to 200 W.

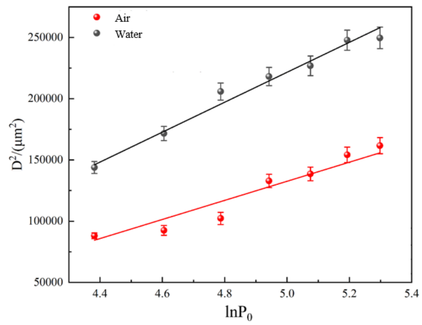

Figure 4. Fitting image of the square of ablative pit diameter and logarithm of average power and ablative threshold.

As shown in Fig.4, the ablation threshold was 12.58 J/cm^2 in air and increased to 22.12 J/cm^2 underwater. At lower power levels, energy loss occurred due to absorption and scattering by the water layer and bubbles, reducing the effective energy reaching the material surface. During this stage, most of the laser energy was consumed by heating, heat transfer, and vaporization of water[17]. Even with increasing power, the majority of energy continued to be spent on vaporizing deionized water until the power exceeded 140 W. Above this threshold, a liquid-free channel formed instantaneously in the interaction zone, minimizing water-related energy attenuation. As a result, the square of the ablation crater diameter increased sharply.

Calculations of the ablation threshold indicated that the computed beam waist radius exceeded the actual beam waist radius of the laser source in both environments. This discrepancy is mainly due to thermal diffusion and heat accumulation effects after the material absorbs laser energy, leading to melt pool expansion. The removal of molten material around the laser interaction zone further amplified this phenomenon. Moreover, the computed beam waist radius was larger in water than in air, which can be attributed to the difference in refractive indices between water and air. Refraction at the air-water interface shifts the focal point downward, thereby increasing the computed beam waist radius.

Material removal was achieved using a high-energy-density laser heat source generated by focusing the laser beam through a lens. The nanosecond laser energy exhibits a Gaussian spatial distribution, with the highest energy density at the focal point. When the laser focus is located on the top surface of the workpiece—defined as the focal plane—the spot diameter is minimized, and the laser intensity is maximized.

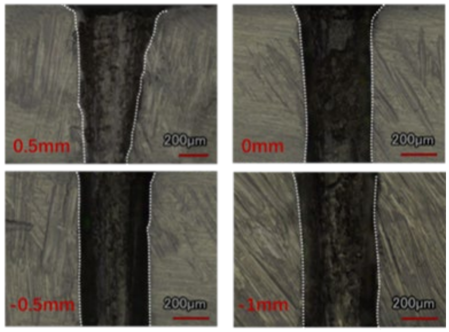

Figure 5. Micro-hole wall morphology corresponding to different focal plane.

In the experiment, the water layer was positioned at the 0.5 mm focal plane. A laser power of 200 W and 30 processing passes were applied, while the defocus distance was varied from -1 mm to +0.5 mm to evaluate its influence on microhole size and morphology.As shown in Fig 5, when a positive defocus distance of +0.5 mm was applied, the microholes exhibited a pronounced tapered shape with relatively poor taper quality. This occurs because the focal point lies above the workpiece surface during machining, resulting in a gradual decrease in laser energy delivery with increasing hole depth. Consequently, material removal in the lower section of the hole becomes insufficient.

When the defocus distance was shifted from +0.5 mm to 0 mm (i.e., focused on the workpiece surface), the exit diameter of the microholes increased noticeably, and the taper decreased significantly—a phenomenon referred to as a “transition effect.” This change is due to the laser spot transitioning from a defocused to a focused state, which concentrates more energy within a smaller area, thereby improving machining accuracy and efficiency.

At a defocus distance of -0.5 mm, where the focal point is located near the center of the workpiece, the microhole sidewall profile was optimal, and the taper was minimal. However, when the defocus was further increased to -1 mm, meaning the laser focus was positioned below the machining surface, the hole wall exhibited broadening. This is caused by the expansion of the laser spot on the workpiece surface, which reduces the energy density per unit area but increases the irradiation zone. The larger interaction area between the laser beam and the workpiece leads to wider hole walls. In addition, the negative defocus condition results in inadequate energy concentration, preventing complete evaporation or effective removal of molten material by the water jet. This leads to partial re-melting and the formation of irregularly widened regions along the hole wall, thereby compromising overall quality [18].

The experimental results indicate that the optimal machining outcome—minimal taper and best microhole quality—is achieved when the laser is focused near the center of the workpiece, corresponding to a defocus distance of approximately -0.5 mm.

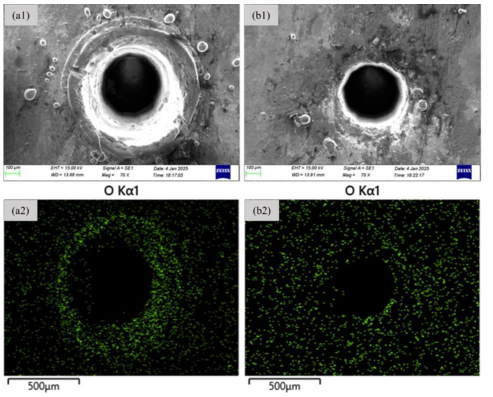

Figure 6. (a) Jet water assistance without delay; (b) Jet water assistance with delay; (1) SEM image of micro-hole entrance morphology; (2) Oxygen element distribution map.

Samples were processed using a waterjet-assisted method combined with a pulse delay strategy for further comparative analysis. Figure 6 shows a comparison of the entrance morphology and oxygen distribution between waterjet-assisted processing without delay and with pulse delay.

As can be seen in Fig. 6(a1), the waterjet-assisted process without delay resulted in a morphology similar to that observed in air processing: significant molten debris (ejecta) around the hole entrance, excessively large and expanded inlet diameter, and a pronounced "bowl-shaped" profile. Although a distinct protruding recast layer—typical of air drilling—was not observed, numerous microcracks were still present. Furthermore, as indicated in Fig. 6(a2), intense oxidation occurred at the entrance under no-delay conditions, resulting in very high oxygen content. This is mainly attributed to the low water layer position and the aggressive laser energy input during the initial stage of blind-hole machining. Repeated laser etching at the hole edge led to severe heat accumulation, irreversible damage to the entrance morphology, and loss of reparability.

After the hole broke through into the second stage, water rapidly rushed in through the outlet, activating new material removal mechanisms. The rapid cooling of the hole wall and entrance induced localized thermal stress, forming additional microcracks. Moreover, due to capillary action, water flowing out from the entrance carried away part of the laser energy, which increased the material removal rate at the inlet region.

In contrast, as shown in Fig. 6(b1), the line delay strategy enabled intermittent energy output from the beginning, thereby controlling the machining intensity. The entrance region expanded less, and the hole opening was better controlled. After breakthrough, the high thermal conductivity of water promoted uniform distribution of laser energy, which facilitated the removal of the recast layer and significantly reduced spatter. The hole wall surface became more uniform, with notably fewer microcracks, leading to a remarkable improvement in hole wall quality. As shown in Fig. 6(b2), the oxygen content at the entrance was very low. The thin flowing liquid film formed on the material surface helped suppress high-temperature oxidation and prevent the formation of excessive oxides.

4. Conclusion

This study optimized waterjet-assisted nanosecond laser drilling of Inconel 718, focusing on pulse delay strategies and key processing parameters. The main findings are:

The line-delay pulse strategy significantly improved microhole accuracy by enabling intermittent energy output, reducing heat accumulation. This minimized entrance diameter, taper, and defects like microcracks.

The ablation threshold of IN718 was higher underwater (22.12 J/cm^2) than in air (12.58 J/cm^2) due to water-induced energy attenuation. Machining efficiency increased above 140 W laser power, where a liquid-free channel enabled direct energy coupling.

Waterjet assistance with pulse delay reduced oxidation and recast layer thickness, improving hole cleanliness and morphology.

This optimized approach effectively produces high-quality microholes in superalloys, showing promise for aerospace applications. Future work will refine delay strategies and extend the technique to other hard-to-machine materials.

Acknowledgements

This work was supported by Qingdao University of Technology, Discipline Innovation and Wisdom Introduction Discipline lnnovation and Wisdom Introduction Base of High-end Laser Intelligent Manufacturing Technology and Equipment, Qingdao University of Technology, Qingdao 266525, China;Shandong Provincial Key Laboratory of High-end Laser Manufacturing Technology and Equipment, Qingdao University of Technology, Qingdao 266525, China

References

[1] T. Zhang, H. Yuan, and M. Cai, "Effects of recast layer on fatigue performance of laser-drilled holes in nickel-based superalloy," J. Mater. Process. Technol. 311, 117821 2023.

[2] S. Ci, J. Liang, J. Li, et al., "Optimizing process for pulsed laser additive manufacturing of nickel-based single crystal superalloy," Mater. Res. Express 10, 096511 2023

[3] K. Pang and D. Wang, "Study on the performances of the drilling process of nickel-based superalloy Inconel 718 with differently micro-textured drilling tools," Int. J. Mech. Sci. 180, 105658 2020.

[4] M. Rahman, A. B. M. A. Asad, and Y. S. Wong, "Introduction to Advanced Machining Technologies," in Comprehensive Materials Processing, Elsevier, 1-13 2014

[5] P. Kuppan, A. Rajadurai, and S. Narayanan, "Influence of EDM process parameters in deep hole drilling of Inconel 718," Int. J. Adv. Manuf. Technol. 38, 74-84 2008

[6] T. J. Chen, B. Q. Yang, B. Li, et al., "Effects of electrochemical corrosion characteristics on electrochemical cold drawing of Q235 steel bar," J. Mater. Process. Technol. 275, 116375 2020.

[7] M. Hasan, J. Zhao, and Z. Jiang, "A review of modern advancements in micro drilling techniques," J. Manuf. Process. 29, 343-375 2017.

[8] D.-W. Kim, M.-W. Cho, T.-I. Seo, et al., "Application of Design of Experiment Method for Thrust Force Minimization in Step-feed Micro Drilling," Sensors 8, 211-221 2008.

[9] P. Singh, A. Pramanik, A. K. Basak, et al., "Developments of non-conventional drilling methods-a review," Int. J. Adv. Manuf. Technol. 106, 2133-2166 2020.

[10] K. P. Rajurkar, M. M. Sundaram, and A. P. Malshe, "Review of Electrochemical and Electrodischarge Machining," Procedia CIRP 6, 13-26 201)

[11] Y. Liu, H. Wang, Z. Zhang, et al., "Laser-liquid composite micromachining technologies: a review of research progress," J. Adv. Manuf. Sci. Technol. 4, 2024002 2024)

[12] H. Wang, Y. Xu, J. Liu, et al., "Magnet-assisted laser hole-cutting in magnesium alloys with and without water immersion," J. Manuf. Process. 61, 539-560 2021

[13] D. Kang, P. Zou, W. Wang, et al., "A lens ultrasonic vibration-assisted laser machining system for laser polishing and laser drilling of 304 stainless steel," Opt. Laser Technol. 144, 107419 2021

[14] K. Xia, N. Ren, Q. Lin, et al., "Femtosecond laser drilling in superalloy with water-based magnetic assistance," Opt. Commun. 527, 128902 2023

[15] H. Wang, Y. Xu, S. Zhu, et al., "Water-based helical laser hole-cutting in nickel super-alloy GH4049 assisted by longitudinal and transverse magnetic fields with/without ultrasonic assistance," Opt. Lasers Eng. 128, 105985 2020

[16] X. D. Wang, A. Michalowski, D. Walter, et al., "Laser drilling of stainless steel with nanosecond double-pulse," Opt. Laser Technol. 41, 148-153 2009

[17] S. Zhu, Y. F. Lu, and M. H. Hong, "Laser ablation of solid substrates in water and ambients," Applied Physics Letters, vol. 79, no. 9, pp. 1396-1398, Aug. 2001.

[18] Y. Zhang, C. Zhang, H. Wang, and et al., "Influence of defocus distance on laser drilling of nickel-based superalloy," Optics & Laser Technology, vol. 135, p. 106678, Mar. 2021.